Opposite Regulation of Insulin Sensitivity by Dietary Lipid Versus Carbohydrate Excess

Anne-Marie Lundsgaard,[1] Kim A. Sjøberg,[1] Louise D. Høeg,[1] Jacob Jeppesen,[1] Andreas B. Jordy,[1] Annette K. Serup,[1] Andreas M. Fritzen,[1] Henriette Pilegaard,[2] Lene S. Myrmel,[3] Lise Madsen,[3,4] Jørgen F.P. Wojtaszewski,[1] Erik A. Richter,[1] and Bente Kiens[1]

Diabetes 2017;66:2583–2595 | https://doi.org/10.2337/db17-0046

To understand the mechanisms in lipid-induced insulin resistance, a more physiological approach is to enhance fatty acid (FA) availability through the diet. Nine healthy men ingested two hypercaloric diets (in 75% excess of habitual caloric intake) for 3 days, enriched in unsaturated FA (78 energy % [E%] fat) (UNSAT) or carbohydrates (80 E% carbohydrate) (CHO) as well as a eucaloric control diet (CON). Compared with CON, the UNSAT diet reduced whole-body and leg glucose disposal during a hyperinsulinemic-euglycemic clamp, while decreasing hepatic glucose production. In muscle, diacylglycerol (DAG) and intramyocellular triacylglycerol were increased. The accumulated DAG was *sn*-1,3 DAG, which is known not to activate PKC, and insulin signaling was intact. UNSAT decreased PDH-E1α protein content and increased inhibitory PDH-E1α Ser^{300} phosphorylation and FA oxidation. CHO increased whole-body and leg insulin sensitivity, while increasing hepatic glucose production. After CHO, muscle PDH-E1α Ser^{300} phosphorylation was decreased, and glucose oxidation increased. After UNSAT, but not CHO, muscle glucose-6-phosphate content was 103% higher compared with CON during the clamp. Thus, PDH-E1α expression and covalent regulation, and hence the tricarboxylic acid cycle influx of pyruvate-derived acetyl-CoA relative to β-oxidation–derived acetyl-CoA, are suggested to impact on insulin-stimulated glucose uptake. Taken together, the oxidative metabolic fluxes of glucose and FA are powerful and opposite regulators of insulin action in muscle.

Excessive ectopic lipid deposition is linked to a number of pathologies, especially insulin resistance, which is a key feature of obesity and type 2 diabetes (1). Yet, the molecular mechanisms responsible for lipid-induced insulin resistance remain poorly understood (2).

Many high-fat feeding studies have been conducted in rats or mice, but a number of the described effects may in part relate to overfeeding and increased adiposity that is observed with high-fat feeding in rodents (3,4). Also, the effect of palmitate incubation, and in a few cases unsaturated fatty acids (FAs), has been investigated in muscle cells; however, often in the context of exposure to high FA concentrations compared with in vivo and after cell culturing in almost FA-free media. Experiments aimed at elucidating the mechanisms in lipid-induced insulin resistance in humans have often used infusion of a lipid emulsion that reduces whole-body and muscle glucose disposal within few hours (5–9). In the field of lipid-induced muscle insulin resistance, the prevailing concept has been that increased FA availability induces accumulation of lipid intermediates, especially diacylglycerol (DAG) (7,10), which causes defects in the proximal insulin signaling, like insulin receptor substrate-1–associated phosphatidylinositol 3-kinase and Akt (11–14). That these mechanisms are responsible for lipid-induced insulin resistance in skeletal muscle of man has been challenged by studies demonstrating no attenuation of insulin signaling after lipid infusions in healthy men (6,8,9,15,16), and furthermore no evidence of a dose-dependent relationship between plasma FA levels and muscle insulin signaling has been found (6). Together, these studies suggest that other mechanisms are involved.

Recent studies have shown that DAG can exist in three different stereo/regio-isomers, each with unique biological

[1]Section of Molecular Physiology, Department of Nutrition, Exercise and Sports, Faculty of Science, University of Copenhagen, Copenhagen, Denmark
[2]Department of Biology, University of Copenhagen, Copenhagen, Denmark
[3]National Institute of Nutrition and Seafood Research, Bergen, Norway
[4]Laboratory of Genomics and Molecular Biomedicine, Department of Biology, University of Copenhagen, Copenhagen, Denmark

Corresponding author: Bente Kiens, bkiens@nexs.ku.dk.

Received 10 January 2017 and accepted 27 July 2017.

This article contains Supplementary Data online at http://diabetes.diabetesjournals.org/lookup/suppl/doi:10.2337/db17-0046/-/DC1.

A.-M.L. and K.A.S. contributed equally to this article.

properties in distinct cell compartments and metabolic pathways. DAG located at the endoplasmic reticulum/Golgi network consists of *sn*-1,2 DAG, which is generated by esterification of glycerol-3-phosphate and fatty acyl-CoA in the glycerol-3-phosphate pathway or the monoacylglycerol acyltransferase reaction during triacylglycerol (TG) synthesis (17), while cytosolic *sn*-1,3 and *sn*-2,3 DAG are mainly generated by lipolysis (18). *Sn*-1,2 DAG located at the plasma membrane is generated from phospholipids. Early studies have shown that PKC is activated solely by *sn*-1,2 DAG isomers and not by *sn*-1,3 and *sn*-2,3 DAG (19–21). So far, only *sn*-1,2 DAG located at the plasma membrane is established to be involved in DAG signaling (17). Thus, the role of DAG in activating PKC and thereby potentially leading to insulin resistance seems to be isoform specific. To our knowledge, no studies have evaluated isoform-specific DAG content in human skeletal muscle.

The lipid-infusion model is an easily accessible approach to induce acute insulin resistance. However, a more physiological human approach would be to enhance FA availability through the diet. Thus, we aimed at clarifying the mechanisms responsible for lipid-induced insulin resistance by feeding healthy individuals a fat-rich diet for 3 days. The duration of the hypercaloric interventions was limited to 3 days in order to investigate the diet-induced molecular mechanisms independent of increased adiposity induced by the overfeeding.

The main focus was on molecular adaptations in skeletal muscle, but as the liver is important in the metabolism of dietary FA and carbohydrates, their effect on hepatic glucoregulation was also considered. As Intralipid and Liposyn infused in most studies consist mainly of unsaturated FA, we designed a diet rich in unsaturated FA in the current study. In order to maximize lipid provision, we provided a high-fat diet in 75% excess of habitual caloric intake. For separation of lipid oversupply from caloric oversupply, the same subjects also consumed a carbohydrate-rich diet for 3 days with matched caloric excess.

For evaluation of underlying molecular mechanisms, biopsies were obtained from skeletal muscle before and after a hyperinsulinemic-euglycemic clamp. Leg arterio-venous catheterization allowed us to measure glucose uptake, and infusion of labeled glucose was applied to evaluate hepatic glucose production in response to the diets. Experiments were conducted after 3 days' randomized consumption of a hypercaloric high-fat diet enriched in unsaturated FA (UNSAT) (78% energy % [E%] fat), a hypercaloric carbohydrate-rich diet (CHO) (80 E% carbohydrates), and a eucaloric control diet (CON). Our hypothesis was that other mechanisms than the canonical insulin signaling pathway are operating in lipid-induced insulin resistance.

RESEARCH DESIGN AND METHODS

Subjects

Nine men were recruited for the study, all healthy and nonsmoking and with no family history of diabetes. The subjects were young (23 ± 3 years old), normal weight (BMI 23.7 ± 1.7 kg · m^{-2}), and moderately trained (maximal oxygen uptake 52 ± 5 mL · kg^{-1} · min^{-1}) (Supplementary Table 1). Informed written consent was obtained prior to inclusion. The study was approved by the Copenhagen Ethics Committee (KF 01 261127). A minor part of the data from the CON and CHO intervention has been presented (22), including selected postabsorptive plasma parameters, as TG, FA, insulin (Table 1), C16:1 n-7 content (Fig. 1), and basal hepatic glucose production (Fig. 2*F*).

Diets

At enrollment, energy content and nutrient composition of the habitual diet were determined from 3 days' weighed dietary registration (Dankost 2000; Dankost, Copenhagen, Denmark). Before provision of the experimental diets, subjects consumed a eucaloric control diet (CON), reflecting their habitual dietary composition (62 E% carbohydrate, 14 E% protein, and 24 E% fat) for 5 days to ensure similar conditions. Subsequently, the two experimental diets (UNSAT and CHO) and the CON diet were provided for 3 days in randomized order, separated by 3 weeks. The UNSAT diet was comprised of 10 E% carbohydrate, 12 E% protein, and 78 E% fat and the CHO diet of 80 E% carbohydrate, 9 E% fat, and 11 E% protein (Supplementary Table 2). The amount of mono- and polyunsaturated FA was partitioned equally in the UNSAT diet. The FA composition of each diet is presented in Fig. 1*A*. All food items were delivered to the subjects under supervision to ensure high compliance. During UNSAT and CHO, subjects were provided a diet in 75% excess of habitual caloric intake and were thus in caloric surplus. The individual daily energy requirement was determined from dietary registrations and prediction equations from Food and Agriculture Organization of the United Nations/World Health Organization.

Experimental Protocol

Experiments were performed after each 3-day intervention. One subject only completed CON and UNSAT owing to personal reasons; hence, n = 8 in CHO. Seventy-two hours before the experimental days, subjects abstained from physical activity. On the experimental days, subjects ingested a light 1.6 MJ meal at 5:00 A.M. at home (Supplementary Table 3) and arrived later at the institute by bus or car. After a period of rest, a venous catheter was inserted into an antecubital vein, and teflon catheters were inserted in the femoral artery and vein. A bolus injection of [6,6-$^2H_2$] glucose tracer (3.203 mg · kg^{-1}) was administered after a blood sample was obtained for determination of background enrichment. Then a constant infusion of labeled glucose (0.055 mg · kg^{-1} · min^{-1}) for 2 h was initiated. Thereafter, subjects underwent a 120-min hyperinsulinemic-euglycemic clamp (1.42 mU insulin · kg^{-1} · min^{-1}), initiated with a bolus injection of insulin (9.0 mU · kg^{-1}) (Actrapid; Novo Nordisk, Denmark). Labeled glucose tracer was added to the glucose infusate to minimize fluctuations in glucose-specific activity (23). Before the clamp start, basal blood samples and biopsies from the vastus lateralis muscle were obtained, which were in the late postabsorptive state 6 h after the meal.

Table 1—Arterial plasma or serum parameters after the control and experimental diets

Arterial plasma or serum parameters	CON	UNSAT	CHO
Glucose, mmol · L^{-1}	5.6 ± 0.2	5.3 ± 0.2*	5.6 ± 0.1
FAs, μmol · L^{-1}	539 ± 60	558 ± 66	175 ± 60**
TG, μmol · L^{-1}	835 ± 118	510 ± 41*	1,681 ± 248***
Epinephrine, mmol · L^{-1}	0.27 ± 0.08	0.35 ± 0.11	0.19 ± 0.06
Norepinephrine, mmol · L^{-1}	1.31 ± 0.48	1.59 ± 0.54	1.56 ± 0.60
Serum tumor necrosis factor α, pg · mL^{-1}	1.64 ± 0.59	1.51 ± 0.32	1.28 ± 0.19*
Serum interleukin-6, pg · mL^{-1}	0.51 ± 0.07	0.54 ± 0.10	0.71 ± 0.13
Serum adiponectin, μg · mL^{-1}	7.1 ± 1.48	6.7 ± 0.13	7.4 ± 1.14
Insulin, μU · mL^{-1}			
Basal	5.0 ± 0.9	6.2 ± 1.8	7.9 ± 1.4*
Clamp	93 ± 3.1###	87.2 ± 4.4###	106.6 ± 4.1###**
C-peptide, pmol · L^{-1}			
Basal	299 ± 31	289 ± 49	377 ± 83(*)
Clamp	203 ± 20###	209 ± 32###	227 ± 37###(*)
HOMA-β, %	45 ± 6	60 ± 8	86 ± 15*
Insulin clearance, mL · kg^{-1} · min^{-1}			
Basal	10.7 ± 2.1	10.8 ± 3.1	8.0 ± 1.8(*)
Clamp	16.0 ± 0.5	17.6 ± 0.8	14.2 ± 0.5*

Data are mean ± SEM and obtained in the late postabsorptive state. The effect of each intervention was compared with CON. For basal variables, a paired *t* test was performed. For variables dependent on time, a two-way RM ANOVA was performed. $n = 9$ in CON and UNSAT; $n = 8$ in CHO. HOMA-β, HOMA of β-cell function. *$P < 0.05$, **$P < 0.01$, ***$P < 0.001$ compared with CON. ###$P < 0.001$ effect of insulin. (*)$P = 0.07$ for C-peptide and $P = 0.06$ for insulin clearance.

Femoral arterial blood flow was determined by ultrasound Doppler (Philips Ultrasound, Bothell, WA). Indirect calorimetry was performed before and during the clamp. Biopsies were obtained from the vastus lateralis muscle before and after 120 min insulin stimulation under local anesthesia.

Analyses

Blood Parameters

The composition of individual FA in plasma was analyzed by combined high-performance liquid chromatography and gas chromatography (Trace Gas Chromatograph 2000; PerkinElmer) as previously described (24). Plasma glucose and lactate concentrations were measured on an ABL615 (Radiometer Medical, Copenhagen, Denmark). The plasma concentrations of FA (NEFA C kit; Wako Chemicals GmbH, Neuss, Germany) and TG (GPO-PAP kit; Roche Diagnostics, Mannheim, Germany) were measured using enzymatic colorimetric methods (Hitachi 912 automatic analyzer; Boehringer Ingelheim, Ingelheim, Germany). Plasma concentrations of insulin and C-peptide were measured by ELISA (ALPCO). Plasma enrichments of the stable glucose isotope were measured using liquid chromatography mass spectrometry (ThermoQuest Finnegan AQA) (25).

Muscle Metabolites

Muscle samples were freeze-dried and dissected free of connective tissue and blood before analyses.

Glycogen content was determined as glycosyl units after acid hydrolysis and measured by a fluorometric method (26), while glucose-6-phosphate (G6P) content was determined after extraction with perchloric acid and measured fluorometrically (26).

Glycogen synthase (GS) activity was measured in muscle homogenates in the presence of 0.03, 0.25, and 12 mmol · l^{-1} G6P, using a Unifilter 350 microtiter plate assay (Whatman, Buckinghamshire, U.K.) (27), modified for microtiter plate assay.

Long-chain FA-CoA was determined by a fluorometric method as previously described (28).

Intramyocellular TG (IMTG), DAG isoforms (*sn*-1,2 and *sn*-1,3 DAG), and ceramide were measured on freeze-dried muscle tissue by thin-layer chromatography. Lipids were extracted under nonheated conditions in chloroform: methanol (2:1, v/v) and dissolved in chloroform before being separated as previously described (29) using *sn*-1,2 and *sn*-1,3 DAG, ceramide, and TG standards from Sigma-Aldrich. Lipid bands were developed at 120°C in 15 min and visualized and quantified by a Kodak Image Station E440 CF (Kodak, Herlev, Denmark). Proper separation of *sn*-1,2 and *sn*-1,3 DAG standards was ensured, and the method was validated for linearity (Supplementary Fig. 1).

Western Blotting

Muscle lysates were prepared, and SDS-PAGE and Western blot analyses were performed as previously described (30). The primary antibodies are described in Supplementary Table 4.

RNA Extraction and Real-time PCR

RNA was isolated from 20 mg wet weight muscle tissue by a guanidinium thiocyanate-phenol-chloroform extraction method (31) with modifications (32), as described in (33). Primers and TaqMan probes were designed using the human-specific Ensemble database (Supplementary Table 5). PDK4 and CPT1 mRNA content were related to the amount of single-stranded DNA, which was similar between groups.

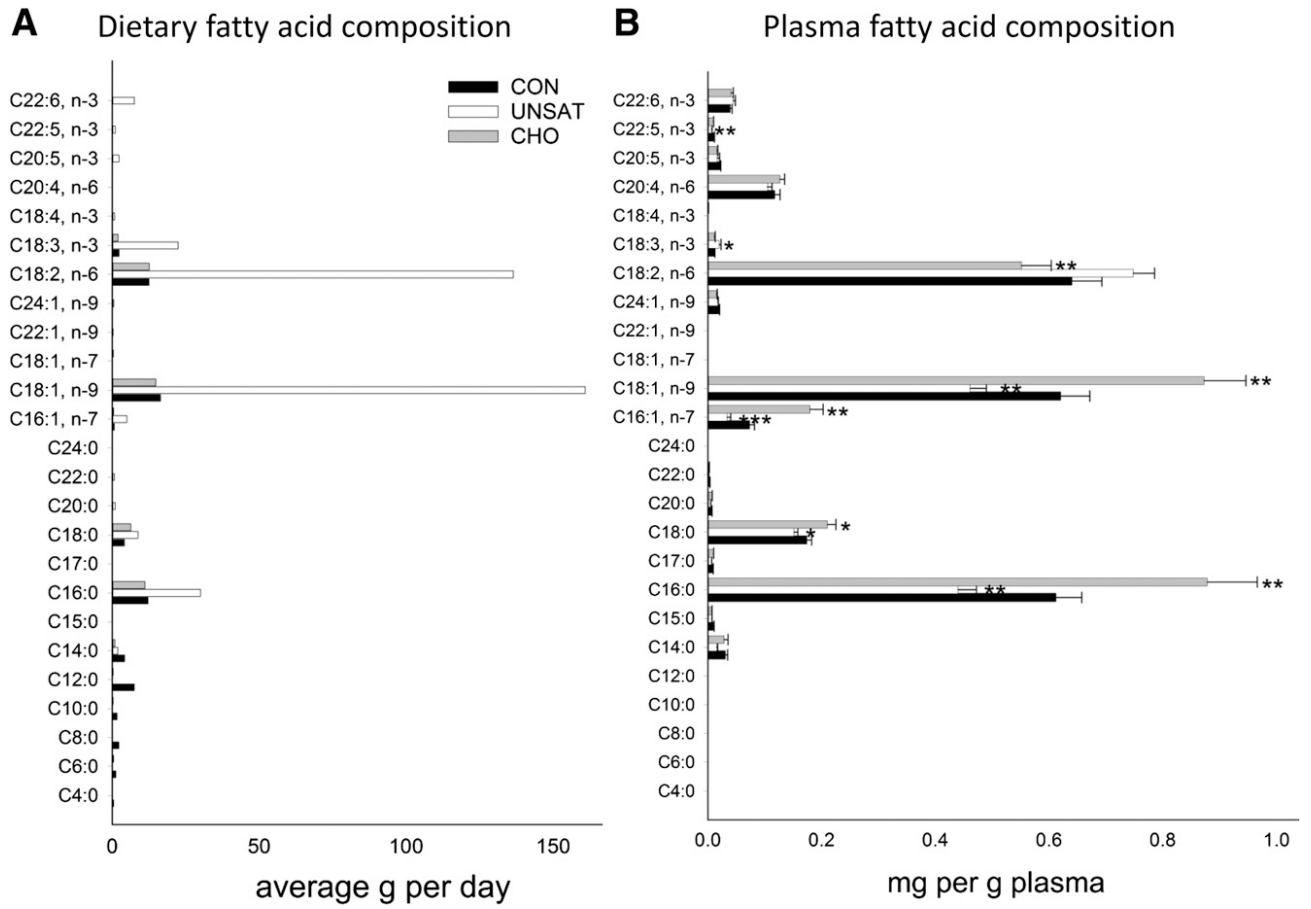

Figure 1—FA composition of the control and experimental diets (*A*) and composition of total FAs in plasma after the respective diets (*B*). The amount of individual FA types in plasma originates from TG and albumin-bound FA. In *A*, the average of the individual FA intakes are in grams per day, with an energy intake of 24.0 ± 0.4 during UNSAT and CHO and 13.7 ± 0.2 MJ during CON. Plasma data are expressed as mean ± SEM and obtained in the late postabsorptive state. $n = 9$ in UNSAT; $n = 8$ in CHO. Thus, $n = 9$ and $n = 8$ in the respective CON bars. *$P < 0.05$, **$P < 0.01$, ***$P < 0.001$ compared with CON.

Calculations

Whole-body insulin sensitivity was expressed as glucose infusion rate per kilogram of body mass. Leg glucose uptake and lactate release were calculated as the arterial-venous difference multiplied by blood flow in accordance with Fick's principle and related to leg mass. The oxidative glucose utilization was calculated from nonprotein VO_2 and VCO_2 (34). All were expressed as the average of the last 60 min of the clamp. Glucose R_a was calculated from the last 20 min of the basal and clamp period using Steele's equation (35). The hepatic insulin resistance index was calculated as glucose $R_{a\ basal} \times [insulin]_{basal}$. HOMA of β-cell was calculated as $20 \times [insulin]_{basal}/[glucose]_{basal} - 3.5$. Basal insulin clearance was calculated as $[C\text{-peptide}]_{basal}/[insulin]_{basal}$. Clamp insulin clearance was calculated as insulin infusion rate/($[insulin]_{clamp} - ([C\text{-peptide}]_{clamp} \times [insulin]_{basal}/[C\text{-peptide}]_{basal})$).

Statistics

Data are means ± SEM. A Shapiro-Wilk test was performed to test for normal distribution. Each experimental trial was compared with CON to test for effect of the experimental diets. For variables independent of time, a paired *t* test was performed. For variables dependent on time, i.e., insulin stimulation, a two-way repeated-measures (RM) ANOVA was performed to test for time and diet effects. Main effects and interactions were evaluated by Tukey post hoc testing. The strength of association between parameters was analyzed using Pearson correlation analysis. A significance level of $P < 0.05$ was chosen. Statistical analyses were performed in SigmaPlot (Systat Software, San Jose, CA).

RESULTS

During the hypercaloric UNSAT and CHO interventions, 24.0 ± 0.4 MJ were provided daily, compared with 13.7 ± 0.2 MJ during CON (Supplementary Table 2). This implied that subjects daily ingested 496 ± 11 g fat and 1137 ± 23 g carbohydrate in UNSAT and CHO, respectively.

Opposite Regulation of Peripheral Insulin Action by Dietary Fat and Carbohydrates

Whole-body insulin sensitivity was reduced 17% after UNSAT ($P < 0.01$) and increased 26% after CHO ($P < 0.01$) compared with CON (Fig. 2*A*). Accordingly, the

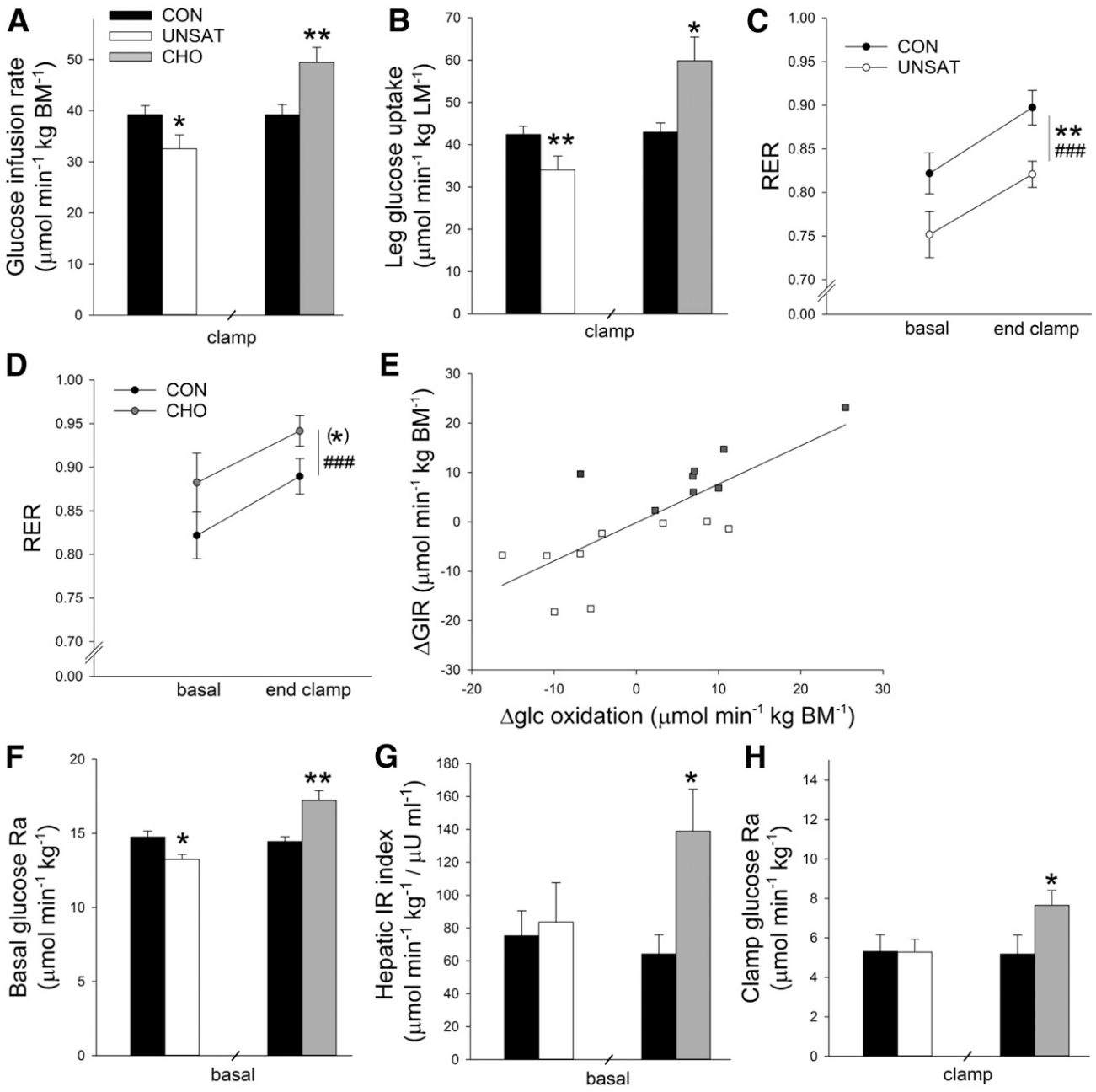

Figure 2—Whole-body and peripheral insulin sensitivity, substrate oxidation, and hepatic glucose production. *A*: Glucose infusion rate expressed per kilogram of body mass (BM). *B*: Insulin-stimulated leg glucose uptake expressed per kilogram of leg mass (LM). In *A* and *B*, values represent the average of the last 60 min of the clamp. *C* and *D*: Whole-body RER values determined from indirect calorimetry before and after 100 min of the clamp. *E*: Scatterplot illustrating the association between the change in glucose (glc) oxidation rate during the clamp and the change (compared with CON) in glucose infusion rate (GIR) after UNSAT (white squares) and CHO (gray squares). *F*: Basal hepatic glucose R_a. *G*: Hepatic insulin resistance (IR) index. *H*: Clamp hepatic glucose R_a during the last 20 min of the clamp. Data are mean ± SEM. The effect of each experimental trial was compared with CON. For variables independent of time, a paired *t* test was performed. For variables dependent on time (*C* and *D*), a two-way RM ANOVA was performed. **P* < 0.05, ***P* < 0.01 compared with CON. ###*P* < 0.001 effect of insulin. (*)*P* = 0.09. *n* = 9 in UNSAT; *n* = 8 in CHO. Thus, *n* = 9 and 8 in the respective CON bars.

insulin-stimulated leg glucose uptake was suppressed 20% after UNSAT ($P < 0.01$) but increased 41% after CHO compared with CON ($P < 0.05$) (Fig. 2*B*). Evaluation of substrate oxidation after UNSAT and CHO revealed oppositely directed changes. The basal respiratory exchange ratio (RER) was 0.82 ± 0.2, 0.75 ± 0.03, and 0.88 ± 0.03 in the CON, UNSAT, and CHO trial, respectively. During the clamp, RER remained lower after UNSAT ($P < 0.01$) and tended to be higher after CHO ($P = 0.067$) (Fig. 2*C* and *D*). The changes in GIR after UNSAT and CHO (calculated as Δ-values compared with CON) were associated with the respective changes in glucose oxidation rate (Fig. 2*E*).

Differential Response of Hepatic Glucoregulation

In contrast to the observation of reduced peripheral insulin sensitivity after UNSAT, the basal hepatic glucose R_a was decreased compared with CON ($P < 0.05$) (Fig. 2*F*) and, hence, fasting plasma glucose was lowered ($P < 0.05$) (Table 1). In contrast, the basal glucose production was increased after CHO ($P < 0.01$) and, hence, the hepatic insulin resistance index was increased ($P < 0.05$) compared with CON (Fig. 2*F* and *G*), contrasting with the higher peripheral insulin sensitivity after this diet. During the clamp, glucose production remained higher after CHO ($P < 0.05$) (Fig. 2*H*), but the relative suppression (%) of glucose production was unchanged. Concomitantly with the higher glucose production, hepatic insulin clearance was lower after CHO during the clamp ($P < 0.05$) (Table 1). Notably, fasting plasma TG was reduced 39% after UNSAT ($P < 0.01$),while being increased 101% after CHO ($P < 0.001$) (Table 1). Analysis of the plasma FA profile revealed a 62% reduction in plasma concentration of palmitoleate C16:1 n-7 after UNSAT ($P < 0.001$) and a contrasting increase by 146% after CHO compared with CON ($P < 0.01$) (Fig. 1*B*). The plasma C16:1 n-7 concentration has been shown to correlate well with D_2O-measured de novo lipogenesis (36), indicating that de novo lipogenesis was decreased after UNSAT and increased after CHO.

Increased *sn*-1,3 DAG and IMTG Content After UNSAT

The basal muscle biopsies were analyzed for the content of different lipid intermediates, in particular, the specific DAG isomers. It was found that almost all DAG was in the *sn*-1,3 isomer form, whereas the *sn*-1,2 (*sn*-2,3) DAG was barely detectable and thus not quantified (Supplementary Fig. 2). After UNSAT, *sn*-1,3 DAG increased by 37% ($P < 0.01$), along with an increase in IMTG content by 52% compared with CON ($P < 0.05$) (Fig. 3*A* and *B*). No changes were observed for long-chain fatty acyl-CoA or ceramide (Fig. 3*C* and *D*). The increased *sn*-1,3 DAG and IMTG content after UNSAT was observed together with a tendency toward increased CD36 protein content ($P = 0.09$) (Fig. 3*E*) (for all proteins or phosphorylations, representative blots are shown in Fig. 6), while the protein content of FABPpm, FATP1, and FATP4 did not change (data not shown). Concomitantly with the increase in *sn*-1,3 DAG, the activating hormone-sensitive lipase (HSL) Ser^{660} phosphorylation was decreased after UNSAT compared with CON ($P < 0.05$),

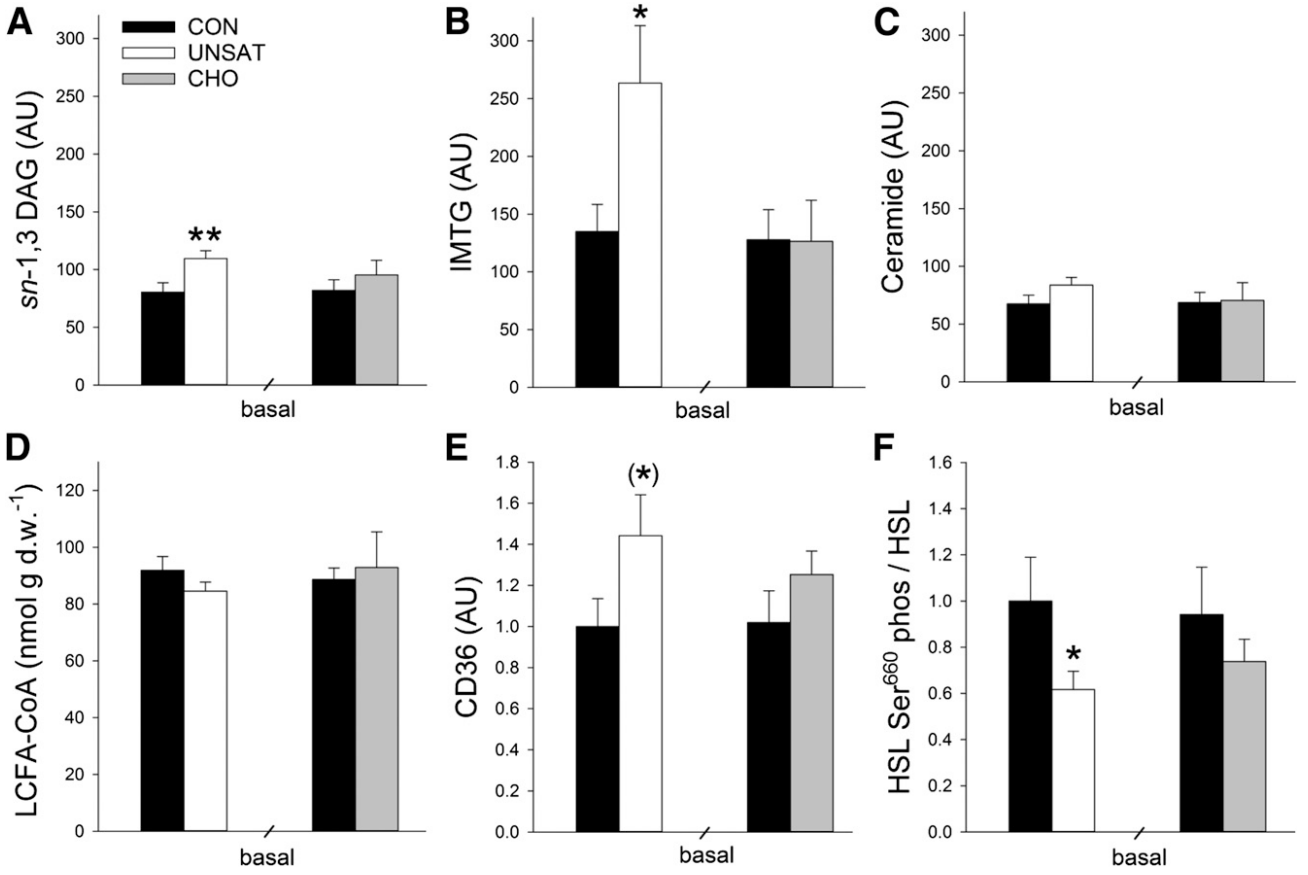

Figure 3—*sn*-1,3 DAG and IMTG content, lipid intermediates, and proteins involved in lipid metabolism in the vastus lateralis muscle, obtained in the late postabsorptive state before the clamp. *A*: *sn*-1,3 DAG content. *B*: IMTG content. *C*: Ceramide content. *D*: Long-chain FA acyl-CoA (LCFA-CoA) content. *E*: CD36 protein content. *F*: HSL Ser^{660} phosphorylation (phos) expressed per total HSL protein. Data are mean ± SEM. The effect of each experimental trial was compared with CON with a paired *t* test. (*)$P = 0.09$, *$P < 0.05$, **$P < 0.01$ compared with CON. $n = 9$ in UNSAT; $n = 8$ in CHO. Thus, $n = 9$ and 8 in the respective CON bars. AU, arbitrary units; d.w., dry weight.

suggesting an attenuated HSL activity and, hence, a reduced DAG hydrolysis. ATGL protein content was not changed. After CHO, no changes in muscle lipid intermediates were obtained.

Insulin Signaling Was Intact After UNSAT

The basal and insulin-stimulated Akt Thr^{308} and TBC1D4 phospho-Akt substrate (PAS) phosphorylation remained unchanged after UNSAT compared with CON (Fig. 4*A* and *B*). The basal protein content of GLUT4 and HKII was not altered after UNSAT (Fig. 4*C* and *D*) and neither were Akt and TBC1D4 proteins. Thus, the reduction in insulin-stimulated glucose uptake was not associated with defects in insulin signaling or the capacity for glucose uptake. After CHO, the increased insulin-stimulated glucose uptake could not be explained by altered insulin signaling (Fig. 4*A* and *B*) and was actually observed despite increased basal muscle glycogen concentration (642 ± 88 mmol · kg d.w.$^{-1}$, where d.w. is dry weight) compared with CON ($P < 0.05$) and a lower basal and insulin-induced glycogen synthase activity ($P < 0.05$) (Fig. 4*E* and *F*).

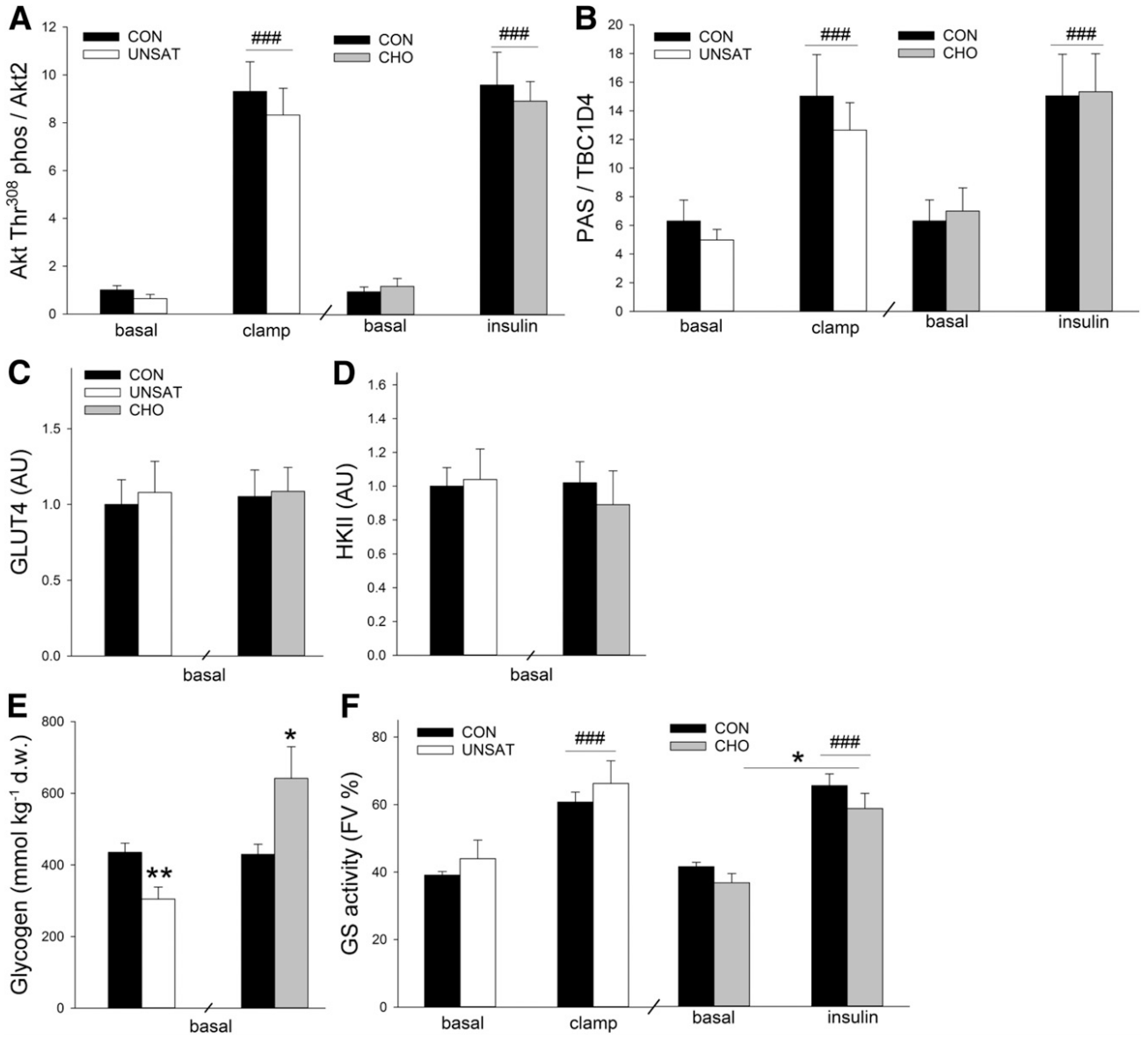

Figure 4—Insulin signaling and proteins involved in glucose metabolism and glycogen synthase activity in the vastus lateralis muscle. Insulin signaling and glycogen synthase activity were evaluated before the clamp and after 120 min of insulin stimulation. *A*: Akt Thr^{308} phosphorylation (phos), expressed per Akt2 total protein. *B*: PAS phosphorylation of TBC1D4, expressed per TBC1D4 total protein content. *C*: GLUT4 protein content. *D*: HKII protein content. *E*: Basal glycogen concentration, given per kilogram of dry weight (d.w.). *F*: GS activity expressed as fractional velocity % (FV %). Data are mean ± SEM. The effect of each experimental trial was compared with CON. For variables independent of time, a paired *t* test was performed. For variables dependent on time (*A*, *B*, and *F*), a two-way RM ANOVA was performed. *P < 0.05, **P < 0.01 compared with CON. ###P < 0.001 effect of insulin. n = 9 in UNSAT; n = 8 in CHO. Thus, n = 9 and 8 in the respective CON bars. AU, arbitrary units.

Decreased Insulin-Stimulated Leg Glucose Uptake Relates to Increased PDH-E1α Phosphorylation and G6P Accumulation After UNSAT

After UNSAT, basal CPT1 mRNA content was increased ($P < 0.01$) (Fig. 5*A*), suggesting an enhanced capacity for mitochondrial FA import. The basal PDK4 mRNA content and PDH-E1α phosphorylation at the inhibitory Ser^{300} site were increased after UNSAT compared with CON ($P < 0.05$) (Fig. 5*B* and *C*), indicating attenuated PDH activity. The total PDH-E1α protein content was also decreased remarkably by 45% after UNSAT ($P < 0.001$), and the proportion of phosphorylated PDH-E1α protein at basal was, hence, even more increased ($P < 0.01$) (Fig. 5*D* and *E*). Remarkably, the diet-induced changes in PDH Ser^{300} phosphorylation remained similar to basal in the insulin-stimulated state (Fig. 5*F*). During the clamp, leg lactate release was increased by 75% in UNSAT ($P < 0.01$) (Fig. 5*G*), indicating a reduced pyruvate conversion to acetyl-CoA. Assessment of the muscle content of G6P in the insulin-stimulated state revealed that G6P was 103% higher after UNSAT compared with CON ($P < 0.05$) (Fig. 5*H*). Accordingly, the increase in PDH Ser^{300} phosphorylation was closely correlated with the reduction in insulin-stimulated leg glucose uptake after UNSAT ($r = -0.97$, $P < 0.001$) (Fig. 5*I*).

After CHO, PDK4 mRNA was decreased ($P < 0.05$) to almost undetectable levels and PDH-E1α phosphorylation per total protein was decreased compared with CON ($P < 0.05$) (Fig. 5*B* and *E*), indicating an increased capacity for entry of pyruvate-derived acetyl-CoA into the tricarboxylic acid cycle. During insulin stimulation, there were no significant differences in G6P compared with CON.

DISCUSSION

One remarkable finding in this study is that insulin-stimulated leg glucose uptake can differ by ~60% after 3 days' dietary manipulation without any detectable changes in insulin signaling, as shown for Akt and TBC1D4 PAS phosphorylation. We here demonstrate that diet-induced manipulation of glucose oxidation and PDH-E1α phosphorylation was remarkably tightly related with changes in leg glucose uptake during insulin stimulation, suggesting that regulation of oxidative glucose disposal can be a strong regulator of insulin action in muscle, independently of insulin signaling.

Increased *sn*-1,3 DAG Accumulation After UNSAT Did Not Interfere With Insulin Signaling

Whole-body insulin sensitivity and insulin-stimulated leg glucose uptake were decreased by 17 and 20%, respectively, after UNSAT compared with CON. The reduction in whole-body insulin sensitivity by dietary FA excess is thus less than the 32–61% reduction obtained with lipid infusion in healthy men (7–9,12,14,15), which is likely related to the circulating FA levels of 1,260–2,370 μmol/L that are acutely induced in the intravenous model. Insulin resistance induced by lipid infusion has in some studies (7,14,37), but not in all studies (8), been associated with muscle DAG accumulation and activation of novel and conventional PKC isoforms, which has been linked to defects in proximal insulin signaling (14). The isoforms of the accumulated DAG were not evaluated in these studies. In the current study, we measured isoform-specific DAG content in human skeletal muscle and showed a 36% increase in *sn*-1,3 DAG content after a short-term hypercaloric diet rich in unsaturated FAs, and this was not associated with reduced insulin-stimulated Akt or TBC1D4 phosphorylation or reduced insulin-induced activation of GS. Cytosolic *sn*-1,3 DAG is generated during TG lipolysis by ATGL, which hydrolyses ester bonds selectively at the *sn*-2 position at TG, while CGI-58 coactivation broadens ATGL activity to *sn*-1, thereby also generating *sn*-2,3 DAG (18). Studies have shown that PKC is activated solely by *sn*-1,2 DAG isomers, and not by *sn*-1,3 and *sn*-2,3 DAG (19–21), thus supporting the intact insulin signaling in the current study. The accumulation of *sn*-1,3 DAG was likely caused by its reduced hydrolysis, due to decreased activity of the DAG lipase HSL, as reflected by reduced HSL Ser^{660} phosphorylation after UNSAT. To this end, unsaturated FAs have also been shown to inhibit HSL activity in a direct manner in vitro (38). The present observations do not exclude that accumulation of *sn*-1,2 DAG, generated during TG synthesis or phospholipid metabolism (17), and subsequent PKC activation, may occur in obesity or other conditions with lipid excess, as in the context of lipid infusion. Investigation of DAG isomer abundance in these conditions is indeed of relevance in future studies.

Increased Phosphorylation of PDH-E1α and G6P Accumulation After UNSAT Relate to Decreased Insulin-Stimulated Leg Glucose Uptake

After UNSAT, RER was lower at basal and during insulin stimulation compared with CON. It was earlier suggested by Randle et al. (39) that an increased FA supply resulted in preferential FA oxidation and reduced glucose oxidation, which subsequently led to reduced glucose uptake. This was described as the "FA syndrome" and initially shown in isolated rat diaphragm and heart (39). Later on, preponderant roles of PDKs and PDH were suggested from in vitro studies. Here, we extend on these findings in human skeletal muscle in a more physiological setting of increased dietary FA availability. Increased unsaturated fat intake increased PDK4 mRNA content, which was paralleled by increased PDH-E1α Ser^{300} phosphorylation both at basal and during the clamp, and a remarkable 45% reduction in PDH-E1α protein, strongly suggesting that PDH activity was attenuated by high fat intake. Additional allosteric regulation of PDH, by altered mitochondrial acetyl-CoA or NADH levels, may also have contributed. A negative correlation was obtained between the increase in PDH Ser^{300} phosphorylation after UNSAT and the decrease in insulin-stimulated glucose uptake ($r = -0.97$, $P < 0.001$). This suggests a mechanism of PDH inhibition after UNSAT, driving the suppression of insulin-stimulated leg glucose uptake. During the clamp, the reduced conversion rate of

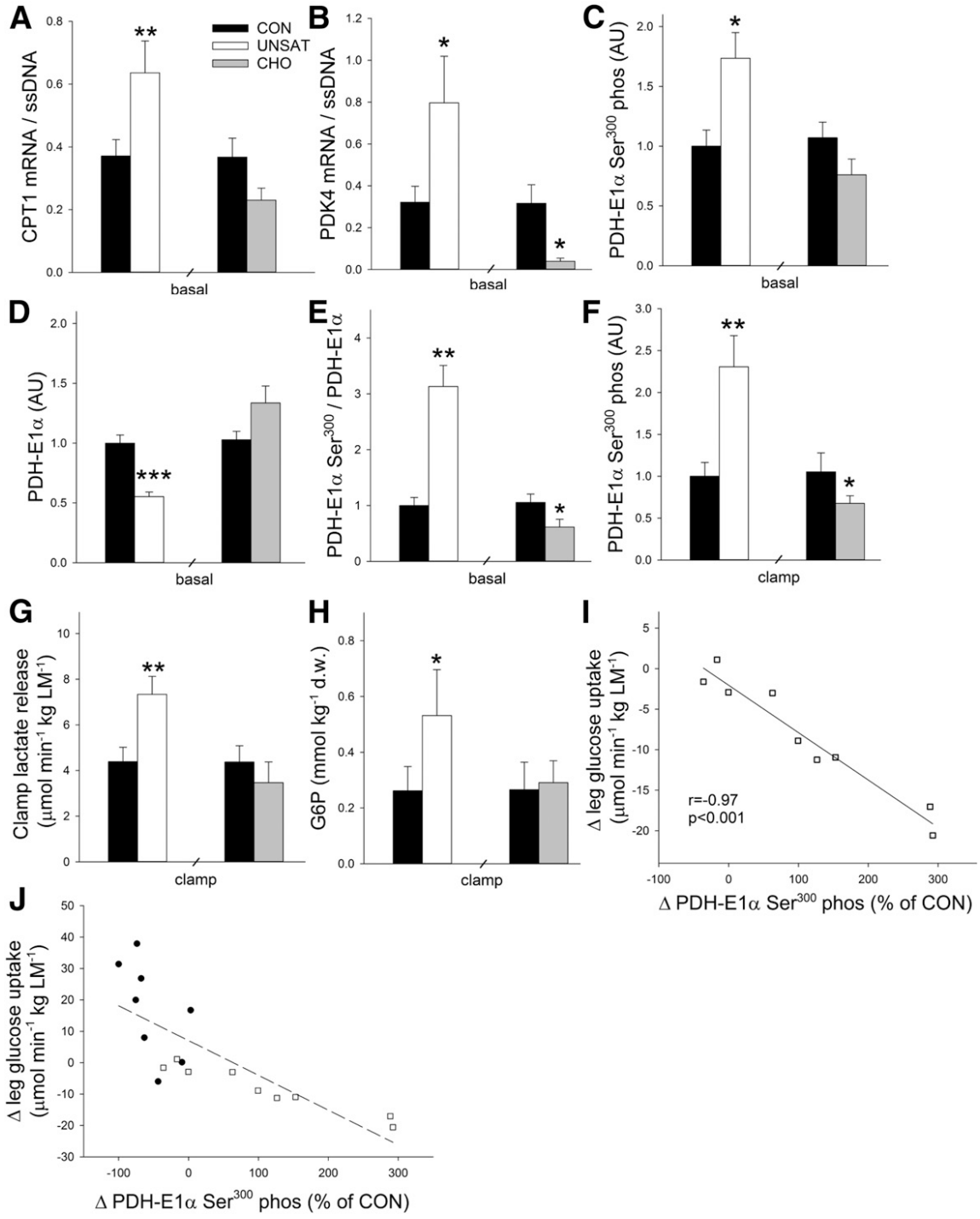

Figure 5—Skeletal muscle CPT1 and PDK4 gene expression, PDH-E1α phosphoregulation, lactate release, and G6P content. *A*: Basal CPT1 mRNA content expressed per single-stranded DNA (ssDNA). *B*: Basal PDK4 mRNA content expressed per ssDNA. *C*: Basal PDH-E1α Ser^{300} phosphorylation (phos). *D*: Basal PDH-E1α protein. *E*: Basal PDH-E1α Ser^{300} phosphorylation expressed per PDH-E1α protein. *F*: PDH-E1α Ser^{300} phosphorylation at the end of the clamp. *G*: Lactate release rate during the clamp expressed per kilogram of leg mass (LM). *H*: G6P content in muscle biopsies obtained at end of clamp, expressed per kilogram of dry weight (d.w.). *I*: Scatterplot illustrating the association between the change in PDH-E1α Ser^{300} phosphorylation and the change in insulin-stimulated leg glucose uptake after UNSAT compared with CON. *J*: Scatterplot illustrating the association between the change in PDH-E1α Ser^{300} phosphorylation and the change in insulin-stimulated leg glucose uptake after both CHO and UNSAT compared with CON. Data are mean ± SEM. The effect of each experimental trial was compared with CON with a paired *t* test. $^{*}P = 0.07$ in *H*; $^{*}P < 0.05$, $^{**}P < 0.01$, $^{***}P < 0.001$ compared with CON. $n = 9$ in UNSAT; $n = 8$ in CHO. Thus, $n = 9$ and 8 in the respective CON bars. $n = 7$ in all groups for mRNA data owing to low RNA yield for two subjects. AU, arbitrary units.

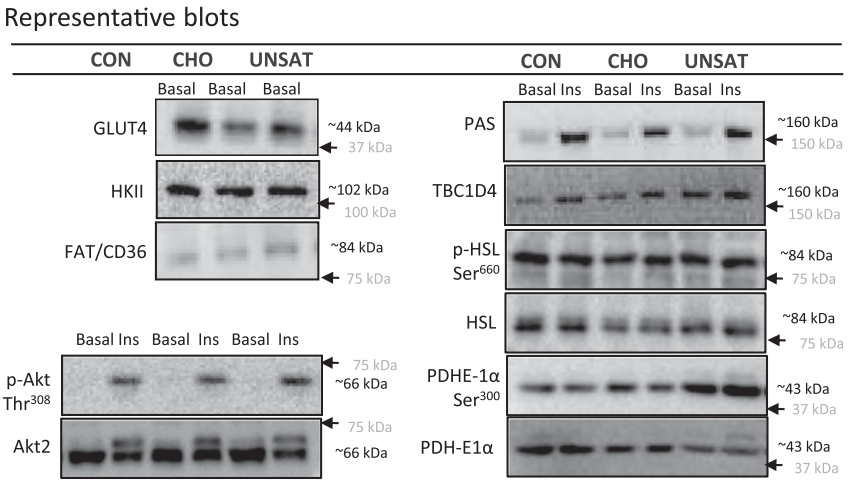

Figure 6—Representative blots from Western blot analyses in skeletal muscle.

pyruvate to acetyl-CoA was evidenced by the increased leg lactate release in UNSAT. The higher muscle content of G6P during the clamp in UNSAT further suggests that carbon influx into glycolysis was attenuated as the upstream result of PDH inactivation. One would expect this backup of glycolysis to inhibit glucose uptake by reducing glucose phosphorylation. This is in contrast to the observations during lipid infusion, where experiments using ^{31}P and ^{13}C MRS have demonstrated that intramuscular G6P content is reduced rather than increased (12,40), which has linked the regulatory mechanisms solely to the step of glucose transport when circulating FA levels are high. The divergence to our findings suggests that when circulating FA levels are very high, as during lipid infusion, the main regulatory step resides at glucose transport. In the more physiological setting as in the current study, our data suggest that the diet-induced inhibition of muscle glucose uptake was more related to a PDH-mediated slowing of glycolysis and accumulation G6P, which in turn could inhibit glucose uptake by inhibition of hexokinase. However, it remains possible that the step of glucose transport was also subject to inhibition and thereby could be a potential additive mechanism in the reduced glucose uptake.

The question is by which mechanisms PDK4 mRNA content was upregulated in UNSAT, leading to inhibition of PDH. Unsaturated FAs are ligands for PPARα and PPARδ (41,42), and in particular FAs liberated by ATGL have this effect (43,44). Hence, in hearts of ATGL$^{-/-}$ mice, PPAR signaling was shown to be lacking and PPAR target genes were reduced (45). During UNSAT, the availability of dietary unsaturated FAs was high and IMTG content increased, while ATGL protein content was maintained. Consequently, liberation of unsaturated FAs from the first lipolytic step by ATGL likely provided ligands for PPAR signaling, evidenced by the increased PDK4 and CPT1 mRNA content.

The concept of lipid-induced regulation of muscle glucose metabolism is summarized and depicted in Fig. 7.

Dietary Carbohydrate Excess Increased Peripheral Insulin Sensitivity

Insulin action was increased after CHO, which is remarkable considering the degree of overfeeding. Thus, the 41% increased insulin-stimulated leg glucose uptake was observed despite a substantial increase in muscle glycogen content, contrasting previous observations (46,45). PDK4 mRNA content was downregulated, possibly mediated by high circulating insulin levels during the intervention, via a phosphatidylinositol 3-kinase–dependent pathway (42), and PDH-E1α Ser^{300} phosphorylation was decreased. Hence, the reduction of fat intake to 11 E% enabled the dietary carbohydrates to trigger glucose oxidation, and together with the lowering of basal plasma FA concentration by 68% ($P < 0.001$) (Table 1), this was a putative mechanism to increase glucose uptake after CHO. It is likely that the increased PDH activation after CHO, and, hence, the increased pyruvate conversion rate, contributed to an efficient carbon influx into glycolysis and oxidation, as no accumulation of G6P was obtained, despite the marked increase in insulin-stimulated glucose uptake.

Differential Effects of Dietary FA and Carbohydrate Excess in the Regulation of Hepatic Glucose Production

The basal glucose production was decreased after UNSAT. Thus, a high fat intake did not adversely affect hepatic glucoregulation even during caloric surplus, at least in the short-term and in healthy subjects. At the same time, the plasma concentration of C16:1 n-7 was decreased after UNSAT compared with CON. This suggests that hepatic de novo lipogenesis was decreased (36), likely related to the lowering of carbohydrate intake to 10 E%. In contrast, glucose production remained higher both at basal and during the clamp after CHO, and the increase in plasma C16:1n-7 concentration indicated an increased de novo lipogenesis. These findings, together with the decreased hepatic insulin clearance, indicate that high carbohydrate intake, when coupled with energy surplus, potentially leads to dysregulated

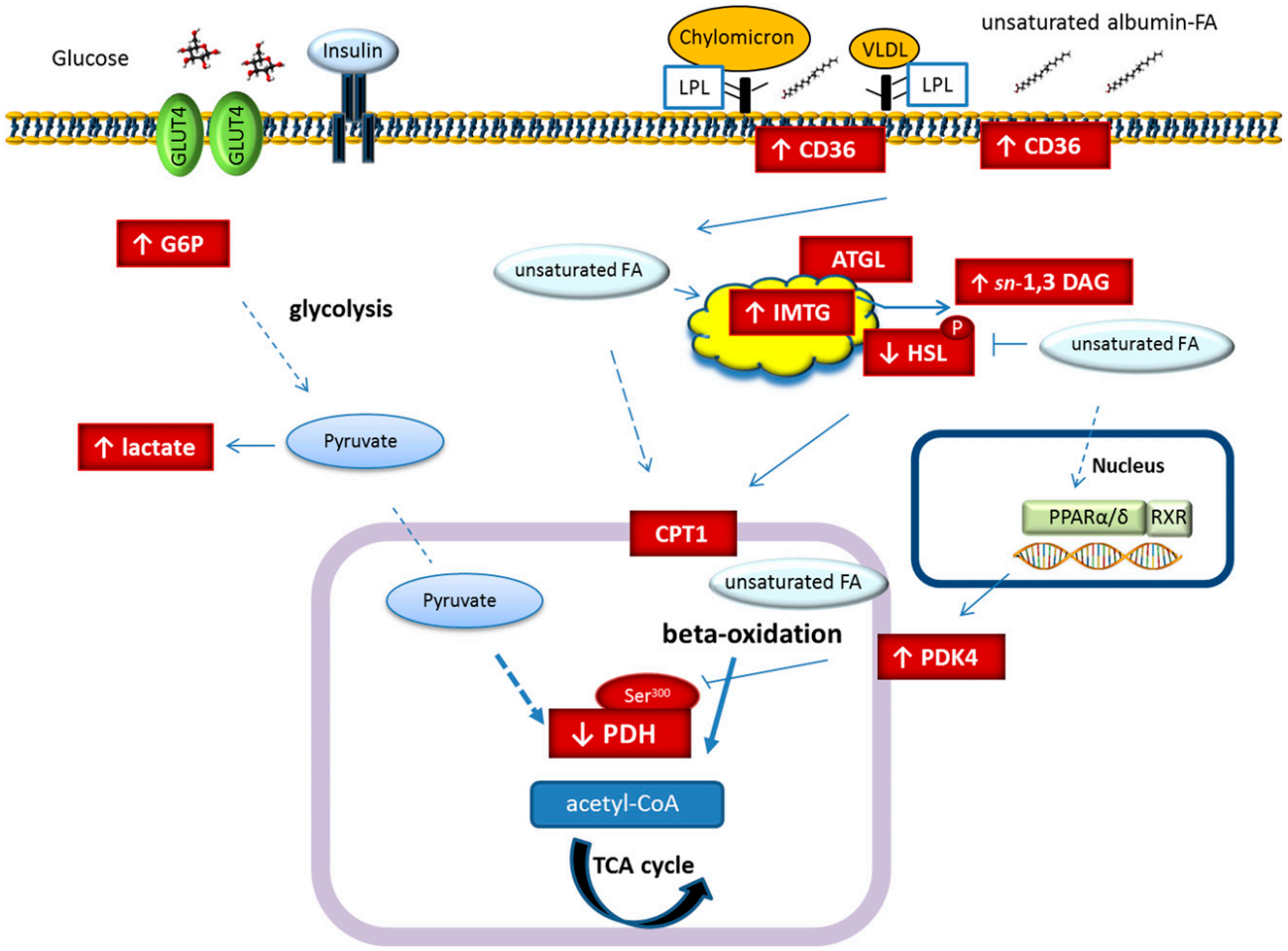

Figure 7—Diagram illustrating the pathways by which unsaturated FAs regulate PDH activity and glucose uptake in skeletal muscle. In the uptake of unsaturated FA, assisted by increased CD36 protein content, the unsaturated FA is to a large extent reesterified and stored in lipid droplets as TG. Subsequent lipolysis by ATGL leads to increased liberation of unsaturated FA, which provides ligands for PPARα and -δ. Activation of PPARs in turn activates transcription of PDK4 and other target genes involved in FA metabolism, e.g., CPT1. PDK4 inhibits the PDH complex by increasing phosphorylation at the Ser^{300} site, favoring increased FA oxidation. Despite an attenuated pyruvate-derived acetyl-CoA influx into tricarboxylic acid, the increased lactate formation indicates that glycolysis is still active, though to a lower extent. Still, G6P accumulates owing to a decreased carbon influx into glycolysis, which in turn leads to decreased glucose phosphorylation. p-Akt, phosphorylated Akt.

hepatic glucoregulation and function, and this may in the long-term change hepatic metabolism in a diabetic direction. We previously showed that the 3-day CHO diet induced an eightfold increase in postabsorptive plasma levels of the hepatic stress sensor FGF21 (22). FGF21 administration in mice has been shown to increase hepatic glucose production, suggesting that FGF21 is a potential mediator of the increase in glucose production after CHO, possibly as a compensatory mechanism to decrease substrate excess in the liver. Concomitantly with the increased de novo lipogenesis, the concentration of plasma TG was increased 101% after CHO. This was likely due to an increased VLDL-TG production, as previously shown after hypercaloric high-carbohydrate provision in healthy subjects (48,49). A decreased hydrolysis of circulating TG, due to insulin-mediated suppression of muscle LPL activity (50) during the intervention, may also have contributed, and potentially explained why IMTG and DAG did not increase as a result of the high plasma TG in CHO.

In conclusion, 3 days' dietary excess of unsaturated FA or carbohydrates had opposing effects on insulin sensitivity in healthy humans. After UNSAT, we demonstrated an enhanced *sn*-1,3 DAG content in muscle, which did not interfere with insulin signaling. Rather, increased phosphorylation of PDH-E1α Ser^{300}, and, hence, decreased PDH activity, was correlated to the reduction in insulin-stimulated leg glucose uptake. The reciprocal aspect was also demonstrated, as CHO decreased PDH-E1α Ser^{300} phosphorylation and increased leg glucose uptake. Thus, the oxidative flux of glucose and FA can be powerful and differential regulators of insulin action. The present data thus show that even dietary unsaturated FAs, that are proposed to be "healthier" than saturated FAs, will induce insulin resistance when consumed in surplus. However, the downregulation of muscle glucose uptake under conditions of high dietary FA availability may reflect an adaptive and reversible response in the present healthy and nonobese subjects rather than a pathological insulin resistance.

In the liver, excess dietary fat (or reduced carbohydrate intake) actually improved hepatic glucoregulation and lowered de novo lipogenesis, while high carbohydrate intake induced hepatic insulin resistance and an increase in plasma TG levels that approached hyper-triglyceridemia. In contrast to the present short-term hypercaloric diet, long-term high carbohydrate intake may, when coupled with excess energy intake, likely lead to a negative regulation of peripheral insulin sensitivity as a result of energy surplus.

Acknowledgments. The authors acknowledge the skilled technical assistance of Irene Bech Nielsen and Betina Bolmgren (University of Copenhagen).

Funding. The study was supported by grants from the Danish Ministry of Food, Agriculture and Fisheries (3304-FSE-06-0510), the Danish Medical Research Council, the Lundbeck Research Foundation (R17-A1760), the Novo Nordisk Research Foundation (13303), and the University of Copenhagen Excellence Program for Interdisciplinary Research (2016) "Physical Activity and Nutrition for Improvement of Health." PhD scholarship of A.-M.L. and a postdoctoral fellowship of A.M.F. were funded by the Danish Diabetes Academy, supported by the Novo Nordisk Foundation. K.A.S. was supported by a postdoctoral research grant from the Council for Independent Research/Medicine.

Duality of Interest. No potential conflicts of interest relevant to this article were reported.

Author Contributions. A.-M.L., K.A.S., L.D.H., J.F.P.W., E.A.R., and B.K. designed the study and carried out the experiments. A.-M.L., K.A.S., L.D.H., J.J., A.B.J., A.K.S., A.M.F., H.P., L.S.M., and L.M. contributed to the results. A.-M.L. and B.K. wrote the manuscript. All authors contributed to the manuscript and approved the final version of the manuscript. B.K. is the guarantor of this work and, as such, had full access to all the data in the study and takes responsibility for the integrity of the data and the accuracy of the data analysis.

References

1. Samuel VT, Petersen KF, Shulman GI. Lipid-induced insulin resistance: unravelling the mechanism. Lancet 2010;375:2267–2277

2. Samuel VT, Shulman GI. Mechanisms for insulin resistance: common threads and missing links. Cell 2012;148:852–871

3. Turner N, Kowalski GM, Leslie SJ, et al. Distinct patterns of tissue-specific lipid accumulation during the induction of insulin resistance in mice by high-fat feeding. Diabetologia 2013;56:1638–1648

4. Hatori M, Vollmers C, Zarrinpar A, et al. Time-restricted feeding without reducing caloric intake prevents metabolic diseases in mice fed a high-fat diet. Cell Metab 2012;15:848–860

5. Bachmann OP, Dahl DB, Brechtel K, et al. Effects of intravenous and dietary lipid challenge on intramyocellular lipid content and the relation with insulin sensitivity in humans. Diabetes 2001;50:2579–2584

6. Gormsen LC, Jessen N, Gjedsted J, et al. Dose-response effects of free fatty acids on glucose and lipid metabolism during somatostatin blockade of growth hormone and insulin in humans. J Clin Endocrinol Metab 2007;92:1834–1842

7. Itani SI, Ruderman NB, Schmieder F, Boden G. Lipid-induced insulin resistance in human muscle is associated with changes in diacylglycerol, protein kinase C, and IkappaB-alpha. Diabetes 2002;51:2005–2011

8. Høeg LD, Sjøberg KA, Jeppesen J, et al. Lipid-induced insulin resistance affects women less than men and is not accompanied by inflammation or impaired proximal insulin signaling. Diabetes 2011;60:64–73

9. Pehmøller C, Brandt N, Birk JB, et al. Exercise alleviates lipid-induced insulin resistance in human skeletal muscle-signaling interaction at the level of TBC1 domain family member 4. Diabetes 2012;61:2743–2752

10. Yu C, Chen Y, Cline GW, et al. Mechanism by which fatty acids inhibit insulin activation of insulin receptor substrate-1 (IRS-1)-associated phosphatidylinositol 3-kinase activity in muscle. J Biol Chem 2002;277:50230–50236

11. Belfort R, Mandarino L, Kashyap S, et al. Dose-response effect of elevated plasma free fatty acid on insulin signaling. Diabetes 2005;54:1640–1648

12. Dresner A, Laurent D, Marcucci M, et al. Effects of free fatty acids on glucose transport and IRS-1-associated phosphatidylinositol 3-kinase activity. J Clin Invest 1999;103:253–259

13. Kruszynska YT, Worrall DS, Ofrecio J, Frias JP, Macaraeg G, Olefsky JM. Fatty acid-induced insulin resistance: decreased muscle PI3K activation but unchanged Akt phosphorylation. J Clin Endocrinol Metab 2002;87:226–234

14. Szendroedi J, Yoshimura T, Phielix E, et al. Role of diacylglycerol activation of PKCθ in lipid-induced muscle insulin resistance in humans. Proc Natl Acad Sci U S A 2014;111:9597–9602

15. Tsintzas K, Chokkalingam K, Jewell K, Norton L, Macdonald IA, Constantin-Teodosiu D. Elevated free fatty acids attenuate the insulin-induced suppression of PDK4 gene expression in human skeletal muscle: potential role of intramuscular long-chain acyl-coenzyme A. J Clin Endocrinol Metab 2007;92:3967–3972

16. Dubé JJ, Coen PM, DiStefano G, et al. Effects of acute lipid overload on skeletal muscle insulin resistance, metabolic flexibility, and mitochondrial performance. Am J Physiol Endocrinol Metab 2014;307:E1117–E1124

17. Eichmann TO, Lass A. DAG tales: the multiple faces of diacylglycerol–stereochemistry, metabolism, and signaling. Cell Mol Life Sci 2015;72:3931–3952

18. Eichmann TO, Kumari M, Haas JT, et al. Studies on the substrate and stereo/regioselectivity of adipose triglyceride lipase, hormone-sensitive lipase, and diacylglycerol-O-acyltransferases. J Biol Chem 2012;287:41446–41457

19. Boni LT, Rando RR. The nature of protein kinase C activation by physically defined phospholipid vesicles and diacylglycerols. J Biol Chem 1985;260:10819–10825

20. Wakelam MJ. Diacylglycerol–when is it an intracellular messenger? Biochim Biophys Acta 1998;1436:117–126

21. Takai Y, Kishimoto A, Kikkawa U, Mori T, Nishizuka Y. Unsaturated diacylglycerol as a possible messenger for the activation of calcium-activated, phospholipid-dependent protein kinase system. 1979. Biochem Biophys Res Commun 2012;425:571–577

22. Lundsgaard AM, Fritzen AM, Sjøberg KA, et al. Circulating FGF21 in humans is potently induced by short term overfeeding of carbohydrates. Mol Metab 2016;6:22–29

23. Molina JM, Baron AD, Edelman SV, Brechtel G, Wallace P, Olefsky JM. Use of a variable tracer infusion method to determine glucose turnover in humans. Am J Physiol 1990;258:E16–E23

24. Lie O, Lambertsen G. Fatty acid composition of glycerophospholipids in seven tissues of cod (Gadus morhua), determined by combined high-performance liquid chromatography and gas chromatography. J Chromatogr A 1991;565:119–129

25. Bornø A, Foged L, van Hall G. Glucose and glycerol concentrations and their tracer enrichment measurements using liquid chromatography tandem mass spectrometry. J Mass Spectrom 2014;49:980–988

26. Lowry OH, Passonneau JV. *A Flexible System of Enzymatic Analysis*. New York, Academic Press, 1972

27. Thomas JA, Schlender KK, Larner J. A rapid filter paper assay for UDPglucose-glycogen glucosyltransferase, including an improved biosynthesis of UDP-14C-glucose. Anal Biochem 1968;25:486–499

28. Antinozzi PA, Segall L, Prentki M, McGarry JD, Newgard CB. Molecular or pharmacologic perturbation of the link between glucose and lipid metabolism is without effect on glucose-stimulated insulin secretion. A re-evaluation of the long-chain acyl-CoA hypothesis. J Biol Chem 1998;273:16146–16154

29. Serup AK, Alsted TJ, Jordy AB, Schjerling P, Holm C, Kiens B. Partial disruption of lipolysis increases postexercise insulin sensitivity in skeletal muscle despite accumulation of DAG. Diabetes 2016;65:2932–2942

30. Fritzen AM, Lundsgaard AM, Jordy AB, et al. New Nordic diet-induced weight loss is accompanied by changes in metabolism and AMPK signaling in adipose tissue. J Clin Endocrinol Metab 2015;100:3509–3519

31. Chomczynski P, Sacchi N. Single-step method of RNA isolation by acid guanidinium thiocyanate-phenol-chloroform extraction. Anal Biochem 1987;162:156–159

32. Pilegaard H, Ordway GA, Saltin B, Neufer PD. Transcriptional regulation of gene expression in human skeletal muscle during recovery from exercise. Am J Physiol Endocrinol Metab 2000;279:E806–E814

33. Fritzen AM, Madsen AB, Kleinert M, et al. Regulation of autophagy in human skeletal muscle: effects of exercise, exercise training and insulin stimulation. J Physiol 2016;594:745–761
34. Frayn KN. Calculation of substrate oxidation rates in vivo from gaseous exchange. J Appl Physiol 1983;55:628–634
35. Steele R. Influences of glucose loading and of injected insulin on hepatic glucose output. Ann N Y Acad Sci 1959;82:420–430
36. Lee JJ, Lambert JE, Hovhannisyan Y, et al. Palmitoleic acid is elevated in fatty liver disease and reflects hepatic lipogenesis. Am J Clin Nutr 2015;101:34–43
37. Nowotny B, Zahiragic L, Krog D, et al. Mechanisms underlying the onset of oral lipid-induced skeletal muscle insulin resistance in humans. Diabetes 2013;62:2240–2248
38. Jepson CA, Yeaman SJ. Inhibition of hormone-sensitive lipase by intermediary lipid metabolites. FEBS Lett 1992;310:197–200
39. Randle PJ, Garland PB, Hales CN, Newsholme EA. The glucose fatty-acid cycle. Its role in insulin sensitivity and the metabolic disturbances of diabetes mellitus. Lancet 1963;1:785–789
40. Roden M, Price TB, Perseghin G, et al. Mechanism of free fatty acid-induced insulin resistance in humans. J Clin Invest 1996;97:2859–2865
41. Forman BM, Chen J, Evans RM. Hypolipidemic drugs, polyunsaturated fatty acids, and eicosanoids are ligands for peroxisome proliferator-activated receptors alpha and delta. Proc Natl Acad Sci U S A 1997;94:4312–4317
42. Abbot EL, McCormack JG, Reynet C, Hassall DG, Buchan KW, Yeaman SJ. Diverging regulation of pyruvate dehydrogenase kinase isoform gene expression in cultured human muscle cells. FEBS J 2005;272:3004–3014
43. Kanaley JA, Shadid S, Sheehan MT, Guo Z, Jensen MD. Relationship between plasma free fatty acid, intramyocellular triglycerides and long-chain acylcarnitines in resting humans. J Physiol 2009;587:5939–5950
44. Dagenais GR, Tancredi RG, Zierler KL. Free fatty acid oxidation by forearm muscle at rest, and evidence for an intramuscular lipid pool in the human forearm. J Clin Invest 1976;58:421–431
45. Haemmerle G, Moustafa T, Woelkart G, et al. ATGL-mediated fat catabolism regulates cardiac mitochondrial function via PPAR-α and PGC-1. Nat Med 2011;17:1076–1085
46. Vendelbo MH, Clasen BF, Treebak JT, et al. Insulin resistance after a 72-h fast is associated with impaired AS160 phosphorylation and accumulation of lipid and glycogen in human skeletal muscle. Am J Physiol Endocrinol Metab 2012;302:E190–E200
47. Derave W, Hansen BF, Lund S, Kristiansen S, Richter EA. Muscle glycogen content affects insulin-stimulated glucose transport and protein kinase B activity. Am J Physiol Endocrinol Metab 2000;279:E947–E955
48. Aarsland A, Chinkes D, Wolfe RR. Contributions of de novo synthesis of fatty acids to total VLDL-triglyceride secretion during prolonged hyperglycemia/hyperinsulinemia in normal man. J Clin Invest 1996;98:2008–2017
49. Mittendorfer B, Sidossis LS. Mechanism for the increase in plasma triacylglycerol concentrations after consumption of short-term, high-carbohydrate diets. Am J Clin Nutr 2001;73:892–899
50. Kiens B, Lithell H, Mikines KJ, Richter EA. Effects of insulin and exercise on muscle lipoprotein lipase activity in man and its relation to insulin action. J Clin Invest 1989;84:1124–1129